Volume 4, Issue 8, August 2014 ISSN: 2277 128X
International Journal of Advanced Research in Computer Science and Software Engineering
Research Paper
Available online at: www.ijarcsse.com

# Diagnose the Thyroid Using Texture Characterization and Classification

**W. R. Sam Emmanuel***
Department of Computer Science & Applications,
Nesamony Memorial Christian College, Marthandam-629165. Tamil Nadu, India

***Abstract— This paper starts with the local textural information of ultrasound thyroid images. The recent feature extraction methods are presented with the different application areas. The basic objective of this study is to identify and represent the performance of a novel approach for texture characterization of thyroid ultrasound images. The method proposed here should reduce the uncertainty produced by the speckle noise in the thyroid images. The Local Binary Pattern (LBP) is extended in the form of fuzzy logic, which allows a Fuzzy Local Binary Pattern (FLBP) helps to improve the performance of thyroid ultrasound images. The training set and testing set are generated from the set of B-scan ultrasound thyroid images in the ratio 80% and 20% respectively. The classification results obtained with the LBP and FLBP are compared with the Gray Level Co-occurrence matrix (GLCM) features using various classifiers.***

***Keywords— Classification, Texture Characterization, LBP, FLBP, Medical Imaging***

## I. INTRODUCTION

The ultrasound (US) is one of the most widely used imaging technologies[1] in medicine. It is portable, free of radiation risk, and relatively inexpensive when compared with other imaging modalities, such as magnetic resonance and computed tomography. The ultrasonography is very useful to detect soft tissue and bony structures. When we deal with superficial organs, the resolution-attenuation limitation does not apply. The texture features and co-occurrence matrix of images play key roles in thyroid detection. The local binary pattern approach and fuzzy local binary patterns are applied with the texture and co-occurrence matrix approaches.

Echographic B-Scan texture[2][30] is the minicomputer based system used to digitize B-mode images and to develop a method to measure their textural information. The information derived from the local histograms is then used to characterize the tissues, to partition the B-mode image into homogeneous zones of texture, to estimate to what extent a tissue is different from another, to delimit the contours of a tissue and to measure its surface. Echographic texture analysis[3] is used for Hashimoto disease. The method was first applied to B-scan images of the normal thyroid and it consistently classified the normal tissue into a unique region. When it is applied to Hashimoto disease B-scan images, the same method segmented the thyroid into two regions. Texture analysis in sonographic images[4] is the study to quantify the sonographic images of the salivary gland to differentiate the Sjogren syndrome (SS) group from the non-SS group. B-scan texture analysis[5] for liver tissue characterization is the diagnostic system for ultrasonic liver tissue characterization based on computerized B-mode image analysis is clinically tested and compared with the results of conventional real-time and static gray scale liver ultrasound as independently assessed by three experienced observers. The diagnostic classes, normal, diffuse parenchymal and malignant disease, are clearly differentiated by computerized image analysis which is superior to subjective evaluation of liver echograms.

The use of image-based machine learning techniques[14] applied in medical image analysis. Some variants of local binary patterns (LBP), which are widely considered the state of the art among texture descriptors. New experiments using several LBP-based descriptors and proposed a set of novel texture descriptors for the representation of biomedical images. Computer-aided detection[6] of prostate cancer is applied for the analysis of transrectal ultrasound images. First, two classifiers based on k-nearest neighbours and Hidden Markov models are compared. Second, the diagnostic capacity of our system is tested by means of a set of experiments where humans with varying degrees of experience classified a set of ultrasound images with and without the aid of the computer-aided system. The corpus used in their study was specifically acquired for this purpose.

Classification based on featured distributions[8] evaluate the performance both of some texture measures which have been successfully used in various applications and of some new promising approaches proposed recently. For classification a method based on Kullback discrimination of sample and prototype distributions is used. The classification results for single features with one-dimensional feature value distributions and for pairs of complementary features with two-dimensional distributions are presented.

Intravascular ultrasound[7] presented the study to evaluate five texture analysis techniques and determine their ability to distinguish between plaque lesions of different composition. Using histological correlation, regions of calcified, fibrous, and necrotic core plaque were chosen from 27 coronary plaques. The analysis of longitudinal ultrasound images[9] are used for aiming at efficient and effective computer-aided detection of thyroid nodules. The proposed scheme involves two phases: a) application of a novel algorithm for the detection of the boundaries of the thyroid gland and b) detection of thyroid nodules via classification of Local Binary Pattern[18][19][20] feature vectors extracted only from the area between the thyroid boundaries. Extensive experiments were performed on a set of B-mode thyroid ultrasound images. The Ultrasound Medical Images can be classified[13] using distance based feature selection and Fuzzy-SVM. This method of classification deals with two important aspects: (i) optimal feature subset selection for representing ultrasound medical images and (ii) improvement of classification accuracy by avoiding outliers. An objective function combining the concept of between-class distance and within-class divergence among the training dataset has been proposed as the evaluation criteria of feature selection. Searching for the optimal subset of features has been performed using Multi-Objective Genetic Algorithm (MOGA). Applying the proposed criteria, a subset of Gray Level Co-occurrence Matrix (GLCM) and Gray Level Run Length Matrix (GLRLM) based statistical texture descriptors have been identified that maximizes separability among the classes of the training dataset. To avoid the impact of noisy data during classification, Fuzzy Support Vector Machine (FSVM) has been adopted that reduces the effects of outliers by taking into account the level of significance of each training sample.

Quantitative image analysis in sonograms of the thyroid gland characterizes thyroid tissue by automatic texture analysis. The texture features that are calculated are based on co-occurrence matrices as they have been proposed by Haralick[23]. The quantitative metric[12] can be used as indirect method for characterization of liver from ultrasound images. This metric is inspired from the visual criterion considered by the radiologists through texture and echogenicity of the Liver in ultrasound image. The proposed metric is a single parameter extracted from 6 texture features on the basis of Homogeneity, Roughness, Contrast, Granularity and Orientation of the liver surface for classification into Fatty or Normal liver.

Local Binary Pattern (LBP)[11][15][16] is a simple yet very efficient texture operator which labels the pixels of an image by threshold the neighbourhood of each pixel and considers the result as a binary number. Due to its discriminative power and computational simplicity, LBP texture operator has become a popular approach in various applications. It can be seen as a unifying approach to the traditionally divergent statistical and structural models of texture analysis. The concept of LBP is applied to Ultrasound Kidney Image Retrieval[21] system. For extracting the texture features from ultrasound kidney images the LBP, rotational invariant LBP and centre symmetric LBP operator is used. The weighted linear filtering approach[10] using Local Binary Patterns (LBP) can be applied for reducing the speckle noise in ultrasound images. The new filter achieves good results in reducing the noise without affecting the image content.

The rest of the chapters are organized as follows. Chapter 2 includes the backgrounds of the different approaches like LBP, GLCM and FLBP, and classification methods. Chapter 3 explained the methodology of the proposed work. It also explains the general procedure and algorithms of LBP, CM and FLBP. Chapter 4 gives the implementation results and discussions. It explains the experimental setup and working with input, the results, and analysis of the results. Chapter 5 explores the performance analysis based on the results obtained followed by the conclusion and feature enhancement presented in the chapter 6.

## II. BACKGROUND

### *A. Local binary pattern*

A local binary pattern (LBP) is a type of feature used for classification in computer vision. The LBP feature extraction method is simple, and efficient for texture analysis. LBP is the particular case of the Texture Spectrum model proposed in 1990. LBP was first described in 1994. It has since been found to be a powerful feature for texture classification[17]; it has further been determined that when LBP is combined with the Histogram of oriented gradients (HOG) classifier, it improves the detection performance considerably on some datasets.

### *B. Gray Level Co-occurrence matrix (GLCM)*

The Co-occurrence matrix method of texture description is based on the repeated occurrence of some gray-level configuration in the texture. A co-occurrence matrix (CM) or co-occurrence distribution is a matrix or distribution that is defined over an image to be the distribution of co-occurring values at a given offset. Co-occurrence matrix captures numerical features of a texture using spatial relations of similar gray tones. Numerical features computed from the co-occurrence matrix can be used to represent, compare, and classify textures.

### *C. Fuzzy Local Binary Pattern*

The Fuzzy Local Binary pattern (FLBP) used to optimize LBP operator and fuzzy threshold for identification of ultrasound images. It is used to handle uncertainty on images with various patterns. FLBP approach is based on the assumption that a local image neighbourhood may be characterized by more than a single binary pattern.

The Local Binary Pattern (LBP) is extended in the form of fuzzy logic, which allows a Fuzzy Local Binary Pattern (FLBP) to help to improve the performance of thyroid ultrasound images. Fuzzy logic was introduced in as a multivalued logic that allows intermediate values to be defined between conventional evaluations like true/false, and high/low.

### *D. Classifications*

Classification approaches like Stochastic Gradient Descent(SGD)[24][25], Support Vector Machines(SVM) [26], Decision Trees(DT) [27] and k-Nearest Neighbour(kNN) [28][29] can be used as Image classifiers. SGD is an approach to discriminative learning of linear classifiers under convex loss functions. The Support Vector Machine (SVM) provides good classification results from complex and noisy data. A support vector machine constructs a hyperplane or set of hyperplanes in a high-dimensional space, which can be used for classification, regression or other tasks. A good separation is achieved by the hyperplane that has the largest distance to the nearest training features of any class (so-called functional margin). The supervised learning method used for classification and regression. The SVM is used to identify the class associated with each pixel. DTs are nonparametric supervised learning methods which create a model that predicts the value of a target variable by learning simple decision rules learned from the data features. The kNN computes the distance between a test point and all points in the training set.

## III. PROPOSED WORK

The researcher adopted to full fill the objectives of the research. The work proposed by the research is explained here.

### *A. Texture Classification*

The classification experiments for the thyroid ultrasound images are done here. The operations performed on 10 patients and 15 ultrasound thyroid images were collected from different patients, which is consider as sample image.

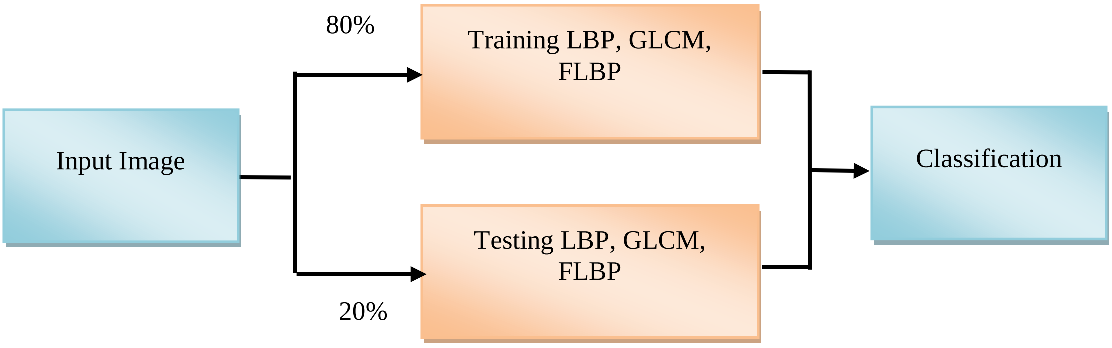


Fig-1 Architectural Design of Texture Classification

The original colour image is converted into the gray scale image. Create 250 images from the sample images by dividing it as 32x32 pixel size. Then collect 80% images from the created sets as training set and remaining will be used as testing set. The constructed training set and testing set are processed separately. The detailed architecture for this classification is shown in Fig-1. The LBP images, FLBP images and co-occurrence matrix(CM) are generated from each of the images. The different texture feature for these LBP, GLCM and FLBP can find out from these images.

Apply different classifiers and compare the classification results. The detailed steps are shown in the algorithm 3.1.

*Algorithm(3.1. General Texture Classification)*

1. *Collect 15 ultrasound thyroid images from different patients, which is considered as sample image.*
2. *Convert the colour images into the gray scale image.*
3. *Create 250 images from the sample images by dividing it as 32x32 pixel size.*
4. *Collect 80% images from the created sets as training set and remaining will be used as testing set.*
5. *Construct the LBP images for the given training set and testing set separately.*
6. *Construct the FLBP images from the training set and testing set separately.*
7. *Find the co-occurrence matrix for training and testing sets.*
8. *Find out the texture features of LBP images.*
9. *Find out the texture features of FLBP images.*
10. *Find the different texture features for the co-occurrence matrix.*
11. *Apply the different classifiers and find out the classification accuracy.*
12. *The classification accuracy of each classifier is analyzed for LBP, GLCM and FLBP.*

### *B. Texture classification using LBP*

The efficient method used for texture analysis is the LBP feature extraction method, which is theoretically and computationally very simple. The LBP feature extraction method [8] was introduced by Ojala et al. in 1996, as a non-parametric, gray-scale invariant texture analysis model, which summarizes the local spatial structure of an image. The LBP operator was represented the local texture around a central pixel based on a 3×3 local neighbourhood. The two possible values zero or one can be assigned based on the value of each peripheral pixels of the neighbourhood and the value of the central pixel. There are $2^8$ total possible LBP codes can defined for the spatial binary patterns with 3×3 pixel neighbourhoods. In the LBP texture representation, a pattern is represented by a set of nine elements $N = \{n_x, n_1, n_2, n_3, n_4, n_5, n_6, n_7, n_8\}$, where $n_x$ represents the intensity value of the central pixel and $n_i, (i = 1...8)$ represent the intensity values of the neighbourhood pixels. The 3×3 neighbourhood can be characterized by a set of binary values $b_i, (i = 1...8)$. The product of the related pixels $n_i, (i = 1...8)$ and $b_i, (i = 1...8)$ generate the LBP value.

 

If the image size 32x32 pixels is considered as input, then take 3x3 local neighbourhoods for each pixel from the 32x32 pixel size image. It is necessary to compute the value of $b_i$ for neighbouring pixel of the center. If the pixel value is greater than or equal to center pixel value then the $b_i$ value is equal to one. If the pixel value is less than the center pixel value then the $d_i$ value is assigned to zero. Here they can express this in the form

$$b_i = \begin{cases} 1 & if \quad n_i \geq n_x \\ 0 & otherwise \end{cases} \tag{1}$$

The LBP value of each pixel is calculated from the binary values of each neighbourhood of the selected pixel. The LBP value is equal to the sum of the product of all neighbouring pixels of $b_i$ and $2^{i-1}$. This can be expressed as

$$LBP = \sum_{i=1}^{8} b_i 2^{i-1} \tag{2}$$

Each and every pixel in an image generates a single LBP code using the related neighbouring pixels. If we combine all the LBP values of each pixel it forms an LBP image. Using the LBP image, the histogram is generated, which collect up the occurrences of different LBP codes from all pixels in the image. This histogram forms the LBP feature vector, which characterize the image texture. The detailed steps and execution flows are explained in the algorithm 3.2.

*Algorithm(3.2. LBP image creation for texture classification)*

1. *Consider the image with 32x32 pixel size as input.*
2. *Take 3x3 local neighbourhoods for each pixel from the 32x32 pixel size image.*
3. *Compute $d_i$ for neighbouring pixel of the center using the following conditions:*

   a) *If the pixel value is greater than or equal to center pixel value then $b_i$ =1.*

   b) *If pixel value is less than the center pixel value then $b_i$ =0.*

4. *Calculate the LBP value for each pixel using the eqn. (2).*
5. *Combine all the LBP values of each pixel it creates an LBP image.*
6. *The histogram for the LBP image will be displayed to show the occurrences of different LBP codes in the image.*

### *C. Co-occurrence Matrix (CM)*

Co-occurrence matrices[22] are quite effective for discriminating different textures but have the disadvantage of a high computational cost. A fast algorithm for calculating parameters of co-occurrence matrices is presented here. The method of co-occurrence has been applied to the problem of classification and segmentation of artificial and natural scenes. For the classification, based on co-occurrence matrix parameters is implemented pixel-by-pixel by using supervised learning and maximum likelihood estimates.

The co-occurrence matrix can measure the texture of the image. Because co-occurrence matrices are typically large and sparse, various metrics of the matrix are often taken to get a more useful set of features. Features generated using this technique is usually called Harlick Features[23].

### *D. Texture Classification using GLCM*

GLCM texture feature is based on the GLCM matrix. The texture is related with the statistical distribution of gray tones. The GLCM is a tabulation $F$ of probability of gray levels i occurring in an image at a distance d in angle $\theta$ from gray level j at points from X and Y. Every entry $c_{ij}$ is a count of the number of times that $F(x, y) = i$ and $F(x+1, y+1) = j$.

For statistical confidence in the estimation of the joint probability distribution, the matrix must contain a reasonably large average occupancy level. Achieved either by (a) restricting the number of amplitude quantization levels (causes loss of accuracy for low-amplitude texture), or (b) using large measurement window (Causes errors if texture changes over the large window). The resultant matrix formed in the form

$$C_{\Delta x, \Delta y}(i, j) = \sum_{x=1}^{n} \sum_{y=1}^{m} \begin{cases} 1 & if\ F(x, y) = i\, and \quad F(x+\Delta x, x+\Delta y) = j \\ 0 & otherwise \end{cases} \tag{3}$$

Where i and j are the image intensity values of the image, x and *y* are the spatial positions in the image $F$ and the offset $(\Delta x, \Delta y)$ depends on the direction. Calculate the mean, variance and standard deviation for the resultant image. Apply different classification methods used for classification. Find out the classification accuracy from the classified result. The histogram for the CM image will be displayed to show the occurrences of different CM codes in the image. The different steps carried out in CM method explained in algorithm 3.3.

 

*Algorithm (3.3. CM image creation for texture classification)*

1. *Get the image $F$ of the size nxm as input.*
2. *Convert the image $F$ into the gray form $F_G$.*
3. *Count the number of times that $F(x,y)=i$ and $F(x+\Delta x, x+\Delta y)=j$ and form the matrix $F_C$ with entries $c_{ij}$.*
4. *Normalize the matrix entries to the estimates of the co-occurrence probabilities and form the matrix $F_N$.*
5. *The resultant matrix is formed using the eqn.(3)*
6. *Find the mean, variance and standard deviation for the resultant image.*
7. *Apply different classification methods to do the classification.*
8. *Find out the classification accuracy.*
9. *The histogram for the CM image will be displayed to show the occurrences of different CM pixels in the image.*

***E. Texture classification using FLBP***

In order to enhance the LBP approach so as to cope with the uncertainty introduced by the speckle noise, the fuzzy logic is considered, as a means to cope with inexactness and improve discrimination power of LBP approach in noise degraded images. Fuzzy logic resembles human decision making, with ability to finding precise solutions in approximate datasets.

The fuzzification of the LBP approach includes the transformation of the input variables to respective fuzzy variables, according to a set of fuzzy rules. To apply the fuzzy approach with LBP, the two fuzzy rules are introduced which describe the relation between the intensity values of the peripheral pixels $n_i$ and the central pixel $n_x$ of a 3×3 neighbourhood.

The input image is considered with the size 32x32 pixels. From the input image take 3x3 local neighbourhoods for each pixel and fix a threshold value T. Compare the intensity value of the neighbourhood pixels $n_i$ with threshold value of the central pixel $n_x$. Apply the fuzzy rules $R_1$ and $R_2$ to describe the relation between the intensity values of the peripheral pixels $n_i$ and the central pixel $n_x$ of a 3x3 neighbourhood. The rules are defined as

$$R_1: \text{if } n_i < n_x \text{ then } b_i = 0$$

$$R_2: \text{if } n_i > n_x \text{ the } b_i = 1$$

The two membership functions $f_1$ and $f_2$ are derived using the rules $R_1$ and $R_2$. The membership function $f_1$ is derived for the peripheral pixels $n_i$ has smaller gray value than the central pixel $n_x$. The membership function $f_2$ is derived for the peripheral pixels $n_i$ has larger gray value than the central pixel $n_x$.

The membership function $f_1$ is considered in three cases: (i) If the peripheral pixels $n_i$ is greater than or equal to the sum of threshold value $T$ and the central pixel $n_x$ then the value of $f_1$ is equal to zero, (ii) if the peripheral pixels $n_i$ is in between the difference of threshold value $T$ and the central pixel $n_x$ and sum of threshold value $T$ then the value of $f_1$ is equal to the sum of the difference between the threshold value and the peripheral pixels $n_i$ and the central pixel $n_x$ is divided by the double of the threshold value $T$, (iii) if the peripheral pixels $n_i$ is less than or equal to the central pixel $n_x$ of minus threshold value $T$ then the value of membership function $f_1$ is equal to one. This is defined as

$$f_1(i) = \begin{cases} 0 & if \quad n_i \geq n_x + T \\ \dfrac{T - n_i + n_x}{2T} & if \quad n_x - T < n_i < n_x + T \\ 1 & if \quad n_i \leq n_x - T \end{cases} \tag{4}$$

The membership function $f_2$ defines the degree to which $n_i$ has a greater gray value than $n_x$, and thus define the degree to which $b_i$ is 1. The membership function $f_2$ is considered in three cases: (i) if the peripheral pixels $n_i$ is greater than or equal to the sum of threshold value $T$ and the central pixel $n_x$ then the value of membership function $f_2$ is equal to one, (ii) if the peripheral pixels $n_i$ is in between the difference of threshold value $T$ and the central pixel $n_x$ and sum of threshold value $T$ then the value of membership function $f_2$ is equal to the sum of the threshold value $T$, the peripheral pixels $n_i$ and the central pixel $n_x$ which is divided by the double of the threshold value $T$, (iii) if the peripheral pixels $n_i$ is less than or equal to the central pixel $n_x$ minus threshold value $T$ then the value of membership function $f_2$ is equal to one. This is defined as

$$f_2(i) = \begin{cases} 1 & if \quad n_i \geq n_x + T \\ \dfrac{T + n_i + n_x}{2T} & if \quad n_x - T < n_i < n_x + T \\ 0 & if \quad n_i \leq n_x - T \end{cases} \tag{5}$$

The membership function $f_2$ is also calculated as

$$f_2(i) = 1 - f_1(i) \tag{6}$$

Calculate the contribution $C_{LBP}$ of each LBP code in a single bin of the FLBP histogram using the 3x3 neighbourhood pixel values using the equation

$$C_{LBP} = \prod_{i=1}^{9} f_{b_i}(i) \tag{7}$$

The total contribution of a 3x3 neighbourhood to the bins of an FLBP histogram is equal to one. The combination of all the FLBP values of each pixel creates an FLBP image. The histogram for the FLBP image will be displayed to show the occurrences of different FLBP codes in the image. The detailed steps are shown in algorithm 3.4.

*Algorithm (3.4. FLBP image creation for texture classification)*

1. *Consider the 32x32 pixel image as input.*
2. *Pick out the 3x3 local neighbourhoods for each pixel from the input image.*
3. *Fix a threshold value $T$.*
4. *Consider the two fuzzy rules $R_1$ and $R_2$ to describe the relation between the intensity values of the peripheral pixels $n_i$ and the central pixel $n_x$ of a 3x3 neighbourhood.*

   $R_1$ *: if* $n_i < n_x$ *then* $b_i = 0$

   $R_2$ *: if* $n_i > n_x$ *the* $b_i = 1$
5. *According to the rules $R_1$ and $R_2$, two membership functions, $f_1$ in eqn. (4) and $f_2$ in eqn. (5) are determined.*
6. *Calculate the 3x3 neighbourhood and find the contribution $C_{LBP}$ of each LBP code in a single bin of the FLBP histogram using the eqn. (7).*
7. *Combine all the FLBP values of each pixel it creates an FLBP image.*
8. *The histogram for the FLBP image will be displayed to show the occurrences of different FLBP codes in the image.*

## IV. RESULTS AND DISCUSSION

The experiment is done with 250 ultrasound scanned images in MATLAB 7.10.0.499(R2010a) application worked in Pentium Dual-Core CPU T4200 at 2GHz RAM. From the experimental set, the 80% (i.e. 200 images) of image data set is considered as training set and the remaining 20% (i.e. 50 images) is considered as testing set. Each of the training and testing sets are individually worked and the LBP, GLCM and FLBP values are computed. The features of LBP, GLCM and FLBP images are extracted and stored in different files for training and testing sets. The features of the training and testing sets are compared with classification results. The classification accuracy of the proposed method is calculated from the detection of thyroid images and normal tissues.

### *A. Experimental Setup*

The data source for the thyroid ultrasound images are taken from different sources of internet. The dataset formed from the collected images. The gray scale images are considered for the experiment. All the images are in Graphics Interchange Format (GIF) formats. The dataset is constructed with 48% (120 images) of normal images and 52% (130 images) of abnormal images. The images are in different sizes between the range of 49KB to 65KB.

### *B. Training Set*

The 80% (ie. 200 images) of image data set is considered as training set. The LBP, GLCM and FLBP features are extracted from the training set; the texture spectrum of histogram features for all the LBP, GLCP and FLBP features are extracted and stored in a file for testing. The sample images used in the training set is displayed in Fig-2.

 

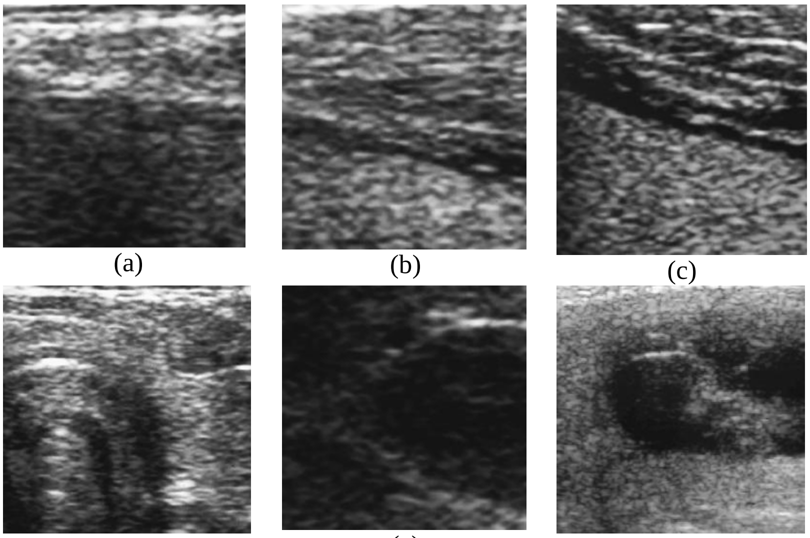

(a) (b) (c)

(d) (e) (f)

Fig-2 Training Set Samples

### *C. Testing set*

The 20% (ie. 50 images) of experimental set is considered for testing. The LBP, GLCM and FLBP features are calculated from the testing set and the texture features like histogram spectrum for all the LBP, GLCM and FLBP are calculated for the related images. The sample images used for testing are displayed in Fig-3.

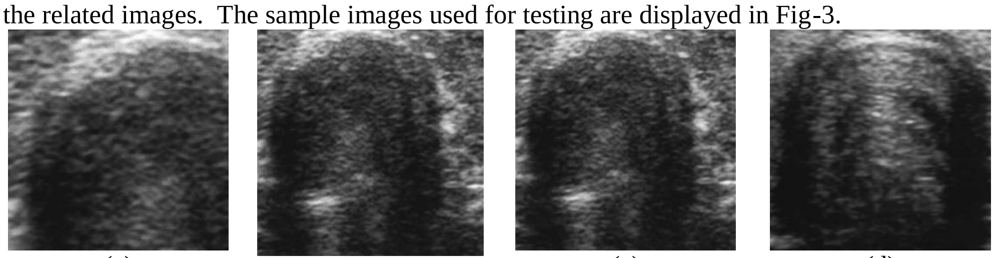

(a) (b) (c) (d)

Fig-3 Testing Set Samples

### *D. Histogram Spectrum*

The texture features of histogram spectrum for the LBP, GLCM and FLBP are shown from Fig-4 to Fig-8. It also shows the histogram differences between the LBP, GLCM and FLBP features.

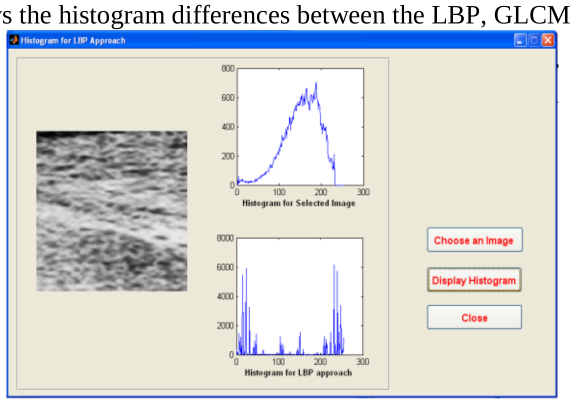


Fig -4 Histogram spectrum feature for LBP approach in normal image

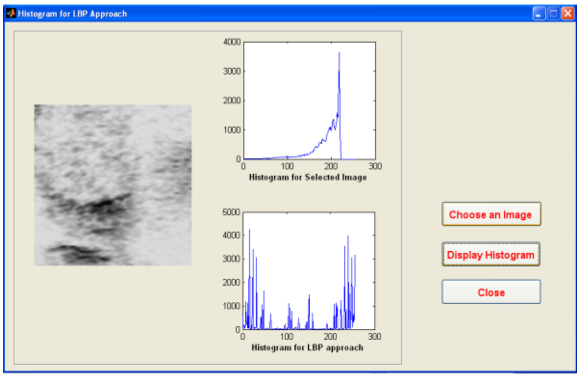


Fig-5 Histogram spectrum feature for LBP approach in nodular tissue

The Fig-4 and Fig-5 illustrate the LBP histograms calculated from blocks sampled from image regions corresponding to normal and nodular tissue respectively. It can be observed that in these histograms out of 255 bins, it has zero values for different bins. This results in a small set of significant peaks that can be identified for each histogram.

The corresponding FLBP histograms are illustrated in Fig-6 and Fig-7. These histograms do not have bins with zero values and there are more spikes, though limited in magnitude. This indicates that FLBP histograms are more informative than LBP histograms. Entropy is a measure of uncertainty associated with the random occurrences, normally considered as the measure of 'disorder'. The Shannon entropy ($\in$) defined in the eqn. (8) is applied here.

$$\in = -\sum_{i=0}^{255} p_i \log(p_i) \qquad (8)$$

 

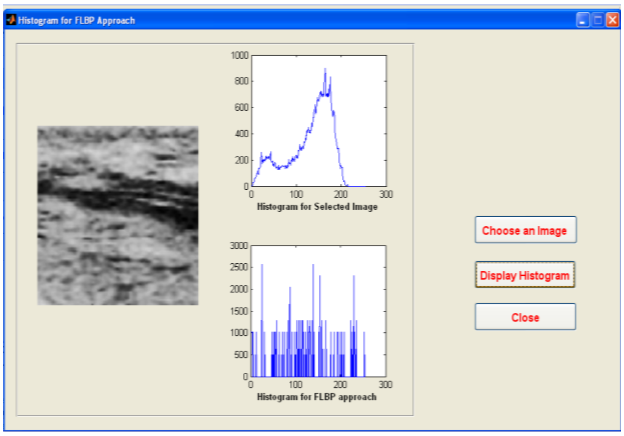


Fig-6 Histogram spectrum feature for FLBP approach in normal image

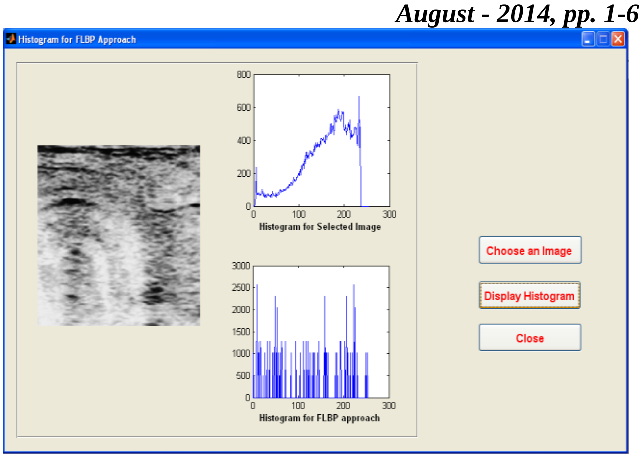


Fig -7 Histogram spectrum feature for FLBP approach in nodular tissue

where $p_i$ is the probability of the i[th] pattern, the more diversified the signal, the higher the entropy, and the more the actual information available. If all the bins have equal probability, the maximum entropy will be reached. Apparently, the FLBP histograms give greater of equal entropy than the crisp LBP histograms. The GLCM histogram gives very poor performance when it compare with LBP and FLBP because there are lot of zeros for various bins. The Fig-8 displays the resultant histogram for the GLCM approach.

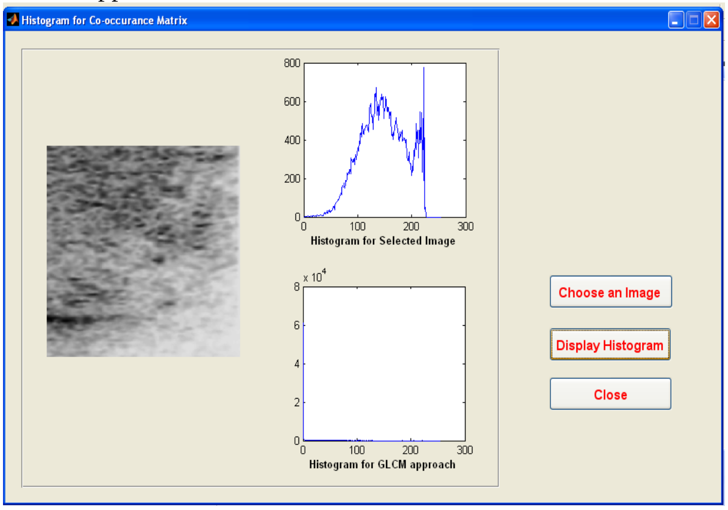


Fig-8 Histogram spectrum feature for GLCM approach

### *E. Classification Results*

The texture features calculated from the LBP image, GLCM image and FLBP image are retrieved from the stored files for the training and testing set. Apply different classification methods SGD, SVM, DT and kNN with the texture features of training and testing set. The classification results for the four classifiers were obtained. The kNN classifiers provides good performance than all other three classifiers for all three approaches, which shown in Fig-9.

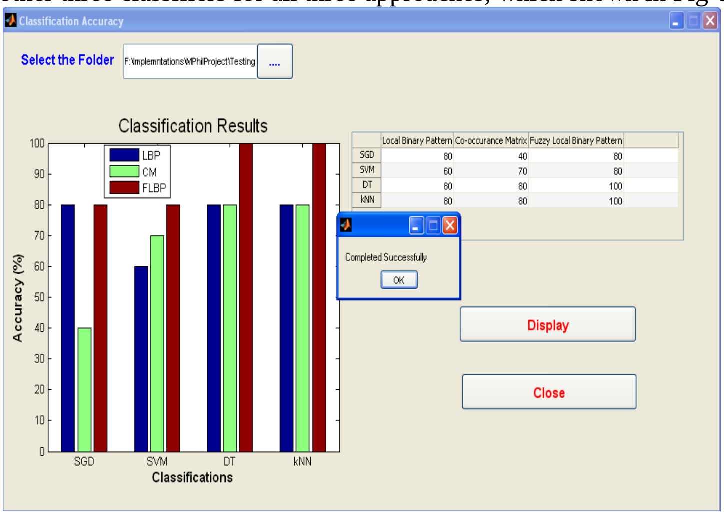


Fig-9 Best classification results obtained with LBP, GLCM and FLBP

 

## V. PERFORMANCE ANALYSIS

To evaluate the performance of the classification of feature extraction techniques, several performance metrics are used here. The classification accuracy is analyzed for the selected classifiers like SGD, SVM, DT and kNN.

### *A. Classification Accuracy*

The classification accuracy is estimated for each approach with different classifiers. The percentage of the accuracy is calculated from the ratio of correctly classified images and the total number of testing images given for classification. The general equation used for the classification accuracy is defined in eqn. (9).

$$CA = \frac{N_{CC}}{N_{TI}} * 100 \quad (9)$$

Where $N_{CC}$ is the number of correctly classified images, $N_{TI}$ is the number of images given for testing.

Table-1 OVERALL CLASSIFICATION ACCURACY IN PERCENTAGE

| **Classifiers** | **LBP** | **GLCM** | **FLBP** |
|---|---|---|---|
| SGD | 80 | 40 | 80 |
| SVM | 60 | 70 | 80 |
| DT | 80 | 80 | 100 |
| kNN | 80 | 80 | 100 |

The results of the different classifiers are compared with various classification results. The Fuzzy Local Binary Pattern approach gives best classification accuracy when comparing with Local Binary Pattern and Gray Level Co-occurrence Matrix. The overall classification accuracy calculated in percentage of correctly classified images shown in Table-1 and the comparative chart displayed in Fig-10. The maximum accuracy for FLBP approach with DT and kNN obtained as 100%. The best results obtained with the LBP reached 80%. Figure-10 shows that the FLBP approach performs better than the LBP and the GLCM approach. The SGD classifier give poor performance for GLCM approach than the LBP and FLBP approaches. The SVM classifier produce good result in FLBP but its performance is poor in LBP and GLCM approaches. The overall performance of the FLBP approach is best for DT and kNN classifiers. If we think over the classifier's performance the kNN give best results, for LBP and GLCM with 80% and FLBP with 100%.

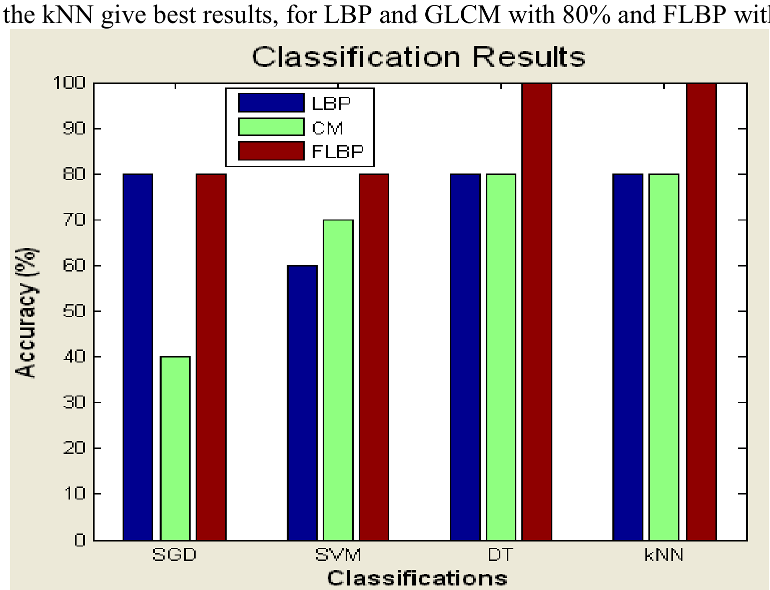


Fig-10 Classification results for different classifiers

### *B. Classification Result with Fuzzification Parameter*

Three FLBP feature sets were extracted by using different values for the fuzzification parameter *T* in the range between zero and 20. For *T*=0, the crisp LBP values were obtained. As a baseline method to compare the classification results obtained by the proposed method they have considered the Gray Level Co-occurrence Matrix (GLCM) approach used in. The best results for the different classifiers are illustrated in Fig-10.

The maximum accuracy obtained is 100% and it was achieved with FLBP features for *T*=3, 4 and 5. The detailed diagram is shown in Fig-11.

 

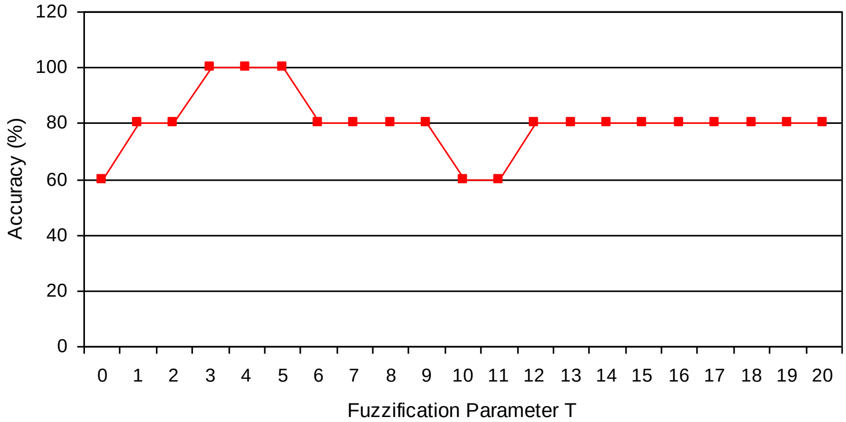


Fig-11 Classification results for different fuzzification parameter

## VI. Conclusions

In this study the Fuzzy Texture Descriptor for Texture Characterization has been used for better representation of textures in ultrasound images. This approach was experimentally evaluated using different classifiers and compared with the LBP and with the co-occurrence matrix approaches on a real dataset of nodular and normal thyroid tissue ultrasound images. As compared to the LBP approach, FLBP approach can improve texture representation in noisy US images. The DT and kNN classifier gives better performance for the FLBP approach.

Investigation of the performance of FLBP approach on ultrasound images acquired from different technology can be classified easily using the kNN of DT classifier. This approach may also helpful to identify different medical diseases using texture features. Instead of using ultrasound images, the video images and colour images also be tested in future.

## References


[1] Bushberg, J.T., The Essential Physics of Medical Imaging, Lippincott Williams & Wilkins, 2002.

[2] Mailloux, G., Bertrand, M., Stampfler, R. and Ethier, S., "Local histogram information content of ultrasound B-mode echographic texture", Ultrasound in Medicine and Biology, Vol. 11, pp.743-750, 1985

[3] Mailloux, G., Bertrand, M., Stampfler, R. and Ethier, S., "Computer Analysis of Echographic Textures in Hashimoto Disease of the Thyroid", Journal of Clinical Ultrasound, Vol. 14, pp.521–527, 1986.

[4] Chikui, T., Okamura, K., Tokumori, K., Nakamura, S., Shimizu, M., Koga, M. and Yoshiura, K., "Quantitative analyses of sonographic images of the parotid gland in patients with Sjögren's syndrome", Ultrasound in Medicine and Biology, Vol. 32, pp.617-622, 2006.

[5] Raeth, U., Schlaps, D., Limberg, B., Zuna, I., Lorenz, A., Kaick, G., Lorenz, W. and Kommerell B., "Diagnostic accuracy of computerized B-scan texture analysis and Conventional ultrasonography in diffuse parenchymal and malignant liver disease", Journal of Clinical Ultrasound, Vol. 13, pp.87-99, 1985.

[6] Llobet, R., Pérez-Cortés, J., Toselli, A. and Juan, A., "Computer-aided detection of prostate cancer", International Journal of Medical Informatics, Vol. 76, pp.547-556, 2006.

[7] Vince, D.G., Dixon, K.J., Cothren, R.M., and Cornhill, J.F., "Comparison of texture analysis methods for the characterization of coronary plaques in intravascular ultrasound images", Computerized Medical Imaging and Graphics, Vol. 24, pp.221–229, 2000.

[8] Ojala, T., Pietikäinen, M., and Harwood, D., "A comparative study of texture measures with classification based on featured distribution" Pattern Recognition, Vol. 29, pp.51-59, 1996.

[9] Keramidas, E.G., Iakovidis, D., Maroulis, D., and Karkanis, S.A., "Efficient and Effective Ultrasound Image Analysis Scheme for Thyroid Nodule Detection", Lecture Notes in Computer Science, Vol. 4633, pp.1052-1060, 2007.

[10] Simily Joseph, "Ultrasound Image Despeckling using Local Binary Pattern Weighted Linear Filtering", 2013.

[11] C.Callins Christiyana, "Comparison of Local Binary Pattern Variants for Ultrasound Kidney Image Retrieval", 2012.

[12] Mandeep Singh, "Quantitative Metric for Liver Classification from Ultrasound Images", 2012.

[13] Abu Sayeed and Md. Sohail, "Classification of Ultrasound Medical Images Using Distance Based Feature Selection and Fuzzy-SVM", 2011.

[14] Loris Nanni, "Local binary patterns variants as texture descriptors for medical image analysis", 2010.

[15] S. Liao, M.W. K. Law, and A. C. S. Chung, "Dominant local binary patterns for texture classification," IEEE Trans. Image Process., vol.18, no. 5, pp. 1107–1118, May 2009.

[16] Z. Guo, L. Zhang, and D. Zhang, "A completed modeling of local binary pattern operator for texture classification," IEEE Trans. Image Process., vol. 19, no. 6, pp. 1657–1663, Jun. 2010.

[17] H. Lategahn, S. Gross, T. Stehle, and T. Aach, "Texture classification by modeling joint distributions of local patterns with Gaussian mixtures," IEEE Trans. Image Process., vol. 19, no. 6, pp. 1548–1557, Jun.2010.

[18] T. Ahonen, A. Hadid, and M. Pietikainen, "Face description with local binary patterns: Applications to face recognition," IEEE Trans. Pattern Anal. Mach. Intell., vol. 28, no. 12, pp. 2037–2041, Dec. 2006.


 

[19] G. Zhao and M. Pietikainen, "Dynamic texture recognition using local binary patterns with an application to facial expressions", *IEEE Trans. Pattern Anal. Mach. Intell.*, vol. 29, no. 6, pp. 915–928, Jun. 2007.

[20] B. Zhang, Y. Gao, S. Zhao, and J. Liu, "Local derivative pattern versus local binary pattern: Face recognition with higher-order local pattern descriptor", *IEEE Trans. Image Process.*, vol. 19, no. 2, pp. 533–544, Feb. 2010.

[21] M. Saadatmand Tarzjan and H. A. Moghaddam, "A novel evolutionary approach for optimizing content based image retrieval", *IEEE Trans. Syst., Man, Cybern. B, Cybern.*, vol. 37, no. 1, pp. 139–153, Feb. 2007.

[22] V. Shah, and S. K. Gandhi, "Image classification based on textural features using artificial neural network", 2012.

[23] Robert M. Haralick, K. Shanmugam, and Its'Hak Dinstein, "Textural features for image classification", vol.3(6), pp.610–621, Nov. 1973.

[24] Y. Tsuruoka, J. Tsujii, and S. Ananiadou, "Stochastic gradient descent training for l1-regularized log-linear models with cumulative penalty", In ACL-IJCNLP 2009, pp.77–485, 2009.

[25] Yuanqing Lin, Fengjun Lv, Shenghuo Zhu, Kai Yu, Ming Yang, and T;Liangliang Cao; Timothee Cour; Huang, "Largescale image classification: fast feature extraction and svm training", In CVPR'11: IEEE Conference on Computer Vision and Pattern Recognition.

[26] V.; Cortes, and C.; Vapnik, "Support-vector networks", Machine Learning, vol.20, pp.273–297, 1995.

[27] L. Breiman, J. H. Friedman, R. A. Olshen, and C.; J. Stone, "Classification and Regression Trees", Chapman Hall, New York, 1984.

[28] A.; Muoz X.; Bosch, and A.; Zisserman, "Scene classification using a hybrid generative/discriminative approach", IEEE Transactions on Pattern Analysis and Machine Intelligence, vol.30(4), pp.712 – 727, April 2008.

[29] Giuseppe Amato and Fabrizio Falchi, "kNN based image classification relying on local feature similarity", In Proceedings of the Third International Conference on Similarity Search and Applications SISAP '10, pp.101–108, 2010.

[30] Dimitris K. Iakovidis, Eystratios G. Keramidas, and Dimitris Maroulis, "Fuzzy Local Binary Patterns for Ultrasound Texture Characterization", Lecture Notes in Computer Science, Vol.5112, pp.750-759, 2008.

 